

Internal collision induced strong-field nonsequential double ionization in molecules

AIHONG TONG,^{1,5} QIANGUANG LI,^{2,5} XIAOMENG MA,³ YUEMING ZHOU,^{3,*} AND PEIXIANG LU^{3,4,6}

¹*Department of Physics and Mechanical & Electrical Engineering, Hubei University of Education, Wuhan 430205, China*

²*School of Physics and Electronic-information Engineering, Hubei Engineering University, Xiaogan 432000, China*

³*School of Physics, Huazhong University of Science and Technology, Wuhan 430074, China*

⁴*Hubei Key Laboratory of Optical Information and Pattern Recognition, Wuhan Institute of Technology, Wuhan 430205, China*

⁵ *These authors contributed equally to this work*

⁶*lupeixiang@hust.edu.cn*

**zhouymhust@hust.edu.cn*

Abstract: Using the classical ensemble method, we have investigated the alignment dependence of the correlated electron dynamics in strong-field nonsequential double ionization (NSDI) of diatomic molecules driven by linearly polarized laser pulses. Our numerical results show that the correlated electron pairs are more likely to emit into the same hemisphere (side-by-side emission) for the parallel aligned molecules at the small internuclear distance, in agreement with previous experimental results. Surprisingly, as the internuclear distance increases, this side-by-side emission is more prevalent for the perpendicularly aligned molecules. Back analyzing of the classical trajectories shows that a considerable part of the NSDI events for the parallel aligned molecules at the large internuclear distances occur through an internal collision, not the well-known recollision. In the internal collision induced NSDI, the first electron tunnels through the inner barrier from the up-field core, moves directly towards the other core, and kicks out the second electron. For this type of NSDI events, the electron pairs are more likely to emit into the opposite hemispheres and thus the correlated electron momentum spectrum exhibits a more dominant back-to-back behavior in the parallel aligned molecules.

© 2019 Optical Society of America under the terms of the [OSA Open Access Publishing Agreement](#)

1. Introduction

As an ideal prototype for investigating electron correlations in strong fields, nonsequential double ionization (NSDI) of atoms and molecules has attracted increasing attention in the strong-field physics community since the first observation of the enhanced yield of doubly charged ions [1,2]. By analyzing the measured recoil ion momentum distributions [3,4], electron energy distributions [5,6], and particularly the correlated electron momentum distributions [7–9], the underlying mechanism of NSDI has been deeply explored. Nowadays it has been widely accepted that strong-field NSDI of atoms and molecules proceeds through a recollision process [10,11], wherein one electron firstly tunnels out of the atom or molecule near the crest of the electric field of the laser pulse, then it is accelerated by the oscillating electric field and impelled back to collide with the parent ion inelastically when the electric field changes its sign, leading to the release of the second electron. In the past decades, a lot of effort has been performed to explore the details of the correlated electron dynamics in the recollision process and the recollision induced process [12,13]. For example, the dependence of NSDI on the driven laser pulses has been comprehensively investigated, and plenty of novel features in correlated electron momentum distributions in NSDI have been observed, through which much detailed dynamics in

the recollision process has been revealed [14–29].

For molecules, there are more degrees of freedom that effect the correlated electron dynamics in NSDI, such as the electron orbits, the molecular alignment, etc. Some of these effects have been experimentally observed [30–33]. For example, subtle difference in the correlated behavior of the electron momentum distributions for NSDI of N_2 and O_2 have been observed experimentally, which has been ascribed to the different orbits of the outmost electrons [30, 31]. For N_2 , it has been experimentally reported that the electron correlation depends on the alignment of the molecules [33], which has been reproduced and explained by theoretical studies [34]. The internuclear distance is another important freedom degree in molecules. In strong-field single ionization (tunneling ionization), it has been shown that the ionization rate sensitively depends on the internuclear distance [35–37]. The ionization rate is greatly enhanced at intermediate nuclear distances. An intuitive physical picture for this enhanced ionization has been proposed. As the internuclear distance increases, an inner potential barrier between the two nuclei appears and then the electron located at the up-field core only needs to tunnel the inner potential barrier to get free. This greatly enhances the tunneling ionization rate. According to this picture, the electron located at the up-field core is more likely to be ionized, which has been confirmed by recent experiment [38, 39]. For NSDI, *ab initio* calculations on hydrogen molecule H_2 have shown that the double ionization yield at the internuclear distance $R = 4$ a.u. is much higher than other values of R , similar to the single ionization [35]. The dynamics for this enhanced double ionization was explained with the simple electrostatic and recollision models [40]. However, the details of the double ionization process and the correlated electron dynamics have not been revealed yet. In this paper, employing the classical ensemble model, we investigate the correlated electron dynamics of NSDI in molecules at different internuclear distances. It is shown that as the internuclear distance increases, the NSDI mechanism changes from the well-known recollision process to an internal-collision process. In this internal-collision process, the first electron emits from the up-field core, moves directly toward the down-field core, and kicks out the second electron. This process leads to the anticorrelated behavior in the final electron momentum distributions. This internal-collision process only occurs for the parallel aligned molecules. Thus, the correlated electron momentum distributions at the intermediate and large nuclear distances for the parallel molecules exhibit a more dominant back-to-back emission behavior, as compared to the perpendicularly aligned molecules. Additionally, we show that the correlation in the electron momentum distribution for this internal collision induced NSDI changes with the internuclear distance.

2. The classical ensemble model

Accurate description of strong-field double ionization requires solving the full dimensional time-dependent Schrödinger equation. However, it requires huge computational resources and is currently only feasible for limited cases [41, 42]. In the past decades, the classical and semiclassical ensemble models have been well established [43–50]. It has been proved that these models are reliable and efficient in investigating strong-field double ionization. They not only reproduced the experimental results but also succeeded in predicting novel features in NSDI [51–54]. Moreover, the underlying dynamics can be revealed by back tracing the classical trajectories [55]. Thus, in this paper, we employ the classical ensemble model to study NSDI of molecules by linearly polarized laser pulses.

In the classical ensemble model, the evolution of the two-electron system is determined by Newton's classical motion equations from beginning to end (atomic units are used throughout this paper unless stated otherwise):

$$\frac{d^2 \mathbf{r}_i}{dt^2} = -\nabla[V_{ne}(\mathbf{r}_i) + V_{ee}(\mathbf{r}_1, \mathbf{r}_2)] - \mathbf{E}(t), \quad (1)$$

where the subscript $i=1, 2$ is the label of the two electrons, and \mathbf{r}_i is the position vector of the i_{th} electron. $V_{ne}(\mathbf{r}_i)$ and $V_{ee}(\mathbf{r}_1, \mathbf{r}_2)$ represent the ion-electron and electron-electron interactions, respectively. $\mathbf{E}(t)$ is an 800 nm linearly polarized laser pulse with a trapezoidal shape, two-cycle turn on, ten cycles at full strength, and two-cycle turn off. Since the investigated electron dynamics of our work usually occurs during one optical cycle, the nuclear motion during this time interval is negligible. Moreover, the fixed-nuclei model is very meaningful and important when one aims to study the R -dependent phenomenon. In this work, the diatomic molecule is aligned along the z axis and two nuclei are fixed at $(0, 0, -R/2)$ and $(0, 0, R/2)$ respectively. So, the parallel and perpendicular alignments of the molecules denote the laser polarization axis is parallel to z and x axes respectively. $V_{ne}(\mathbf{r}_i) = -1/\sqrt{x_i^2 + y_i^2 + (z_i - R/2)^2 + a^2} - 1/\sqrt{x_i^2 + y_i^2 + (z_i + R/2)^2 + a^2}$ and $V_{ee}(\mathbf{r}_1, \mathbf{r}_2) = 1/\sqrt{(x_1 - x_2)^2 + (y_1 - y_2)^2 + (z_1 - z_2)^2 + b^2}$, where the soft-core Coulomb potential is employed. We have set $a = 1.25$ to avoid autoionization and $b = 0.05$ to prevent numerical singularity [43].

To obtain the initial values for Eq. (1), the ensemble is populated starting from a classically allowed position for the ground state energy of the target molecule. In our calculations, we select H_2 as the target molecule and study double ionization at different internuclear distances $R = 2$ a.u., 4 a.u. and 6 a.u. The corresponding ground state energies are -1.67 a.u., -1.26a.u. and -1.17a.u. respectively [56]. Qualitatively, the results of our calculations are general for other diatomic molecules and the results are insensitive to the ionization potential. Given the positions of two electrons, the kinetic energy of two electrons is the difference between the ground state energy and the potential energy of the system. This available kinetic energy is randomly distributed between the two electrons. Then the electrons are allowed to evolve for a sufficient long time (100 a.u.) in the absence of the laser field to obtain stable position and momentum distributions, which are the initial ensemble for Eq. (1). The double ionization event is determined if the energies of the two electrons are positive at the end of the laser pulse.

3. Results and discussions

Figure 1 shows the correlated electron momentum spectra along the laser polarization direction for NSDI of H_2 with $R = 2$ a.u. (first column), 4 a.u. (second column) and 6 a.u. (third column), respectively. In the first and second rows, the molecules are aligned parallel and perpendicular to the laser polarization direction, respectively. For $R = 2$ a.u., the NSDI events for the parallel molecules mainly distribute in the first and third quadrants, showing the dominant side-by-side emissions. For the perpendicularly polarized molecules, more NSDI events move to the second and fourth quadrants, as shown in Figs. 1(a) and 1(d). It indicates that the two electrons are more likely to emit into the same direction when the molecule is parallel to the laser polarization direction. This is in well agreement with the previous experimental results [33]. It has been explained that this behavior is attributed to the difference between the suppressed potential barriers of parallel and perpendicular molecules. In the perpendicular alignment, the potential barrier is wider and higher, and thus the second electron is detached with a long time delay after recollision, as compared with the parallel alignment [34]. Thus, the back-to-back emission is more prevalent in the perpendicularly aligned molecules. As R increases, the distribution in the second and fourth quadrants decreases for the perpendicularly aligned molecules, as shown in Figs. 1(d)-1(f). This is because that the ionization potential decreases with the increasing R and thus more events occur through the recollision-impact ionization pathway.

More interesting results could be seen when diagnosing the alignment dependence of the correlated electron spectra. It is shown that the alignment dependence of the correlated electron momentum distributions is totally different from that at the smaller R . For example, at $R = 4$ a.u., the electron pairs exhibit the side-by-side emissions for the perpendicular alignment [Fig. 1(e)]. However, for the parallel alignment, the proportion of the back-to-back emission increases

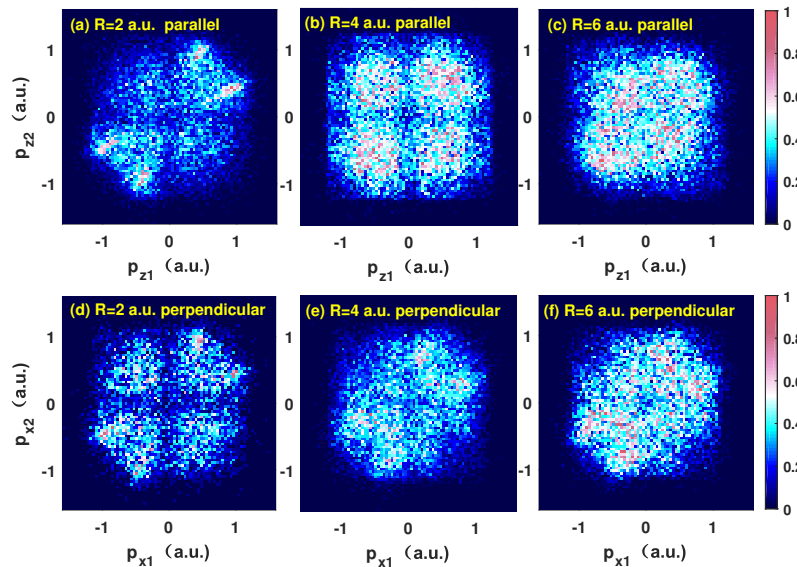


Fig. 1. Correlated electron momentum spectra along the laser polarization direction for NSDI of H_2 at $\lambda = 800$ nm, $I = 1.0 \times 10^{14} W/cm^2$. The molecules are aligned parallel and perpendicular to the laser polarization direction for the first and second rows, respectively. The internuclear distances of the molecules from the first to the third columns are 2 a.u., 4 a.u., and 6 a.u., respectively. In the calculation, the ensemble sizes of (a)-(f) are 2.00, 0.20, 0.20, 8.00, 2.00, and 2.00 million, resulting in more than twenty thousand NSDI events for statistics in each spectra.

obviously and the correlated electron momentum spectrum appears an almost uniform distribution in the four quadrants, as shown in Fig. 1(b). The situation is similar at $R = 6$ a.u., as shown in Figs. 1(c) and 1(f). These results indicate that the electron pairs for the parallel alignment are more likely to emit to the opposite hemispheres, as compared to the perpendicular alignment. It is in contrast with the case at the smaller internuclear distance, implying the different ionization dynamics.

To disclose the underlying ionization dynamics for this alignment-dependent correlation at $R = 4$, and 6 a.u., we trace the NSDI classical trajectories, and find that besides the well-known recollision process, a considerable part of the NSDI events for the parallel aligned molecules at $R = 4$ a.u. (15%) and $R = 6$ a.u. (34%) occur through an internal-collision process. In the left and right columns of Fig. 2 we present two sample trajectories of the recollision and internal collision induced NSDI in the parallel aligned molecules with $R = 6$ a.u., respectively. The first and second rows show the time evolution of the z -coordinate (along laser polarization direction) and the energy of the two electrons. For the recollision trajectories (left), one electron is first set free by the laser field and moves away from the core, and it is driven back about $0.5T$ (T is the cycle of the laser field) later. Then recollision occurs where the energy exchange is obvious, as indicated by the black arrow in Fig. 2(b). This is a typical recollision trajectory of NSDI. After recollision, the two electrons emit into the same direction along the laser polarization, as shown in Fig. 2(c) where the electron trajectories in the x - z plane are shown. For the trajectory in the right column, the electron moves from one core to the other core (the red one), and a collision occurs after which one electron is released (the blue one), and the other electron emits at the next crest of electric field. We refer this trajectory as the internal collision induced NSDI. For this trajectory, the two electrons finally emit into the opposite directions along the laser polarization,

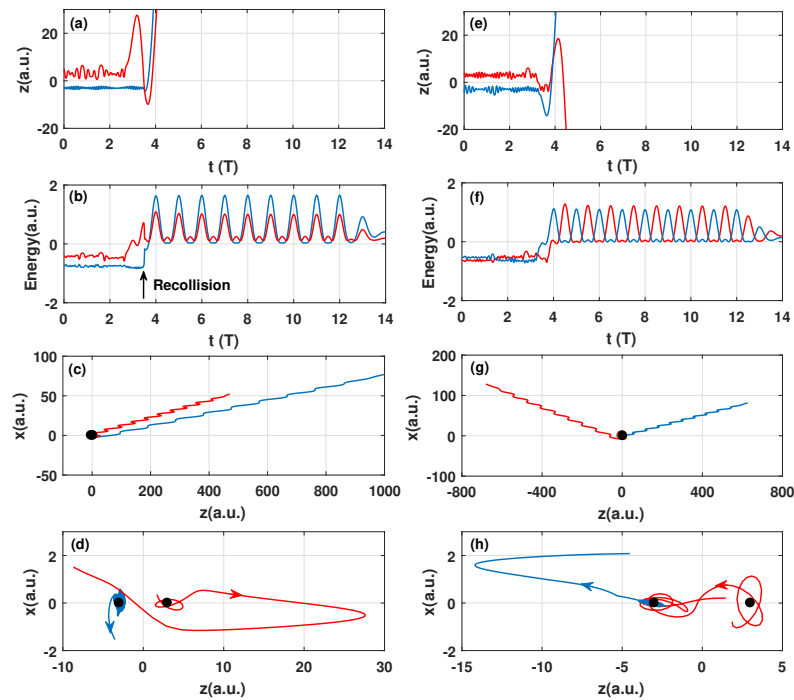


Fig. 2. Two sample trajectories of NSDI for the parallel molecule with $R = 6$ a.u. Left column, the trajectory of recollision induced NSDI. Right column, the trajectory of the internal collision induced NSDI. The first and second rows show the time evolution of the z -component coordinate and the energy of the two electrons. The third row displays the trajectories of electrons in x - z plane and the fourth row zooms in the behavior of the trajectories near the core. The black arrow in (b) indicates the recollision.

as shown in Fig. 2(g). In the bottom line of Fig. 2, we zoom in these two trajectories near the core, wherein the electron dynamics is more intuitive displayed.

In order to identify whether the internal-collision process is responsible for the enhanced back-to-back emissions in Figs. 1(b) and 1(c), we separately display the correlated electron momentum spectra for the recollision and internal-collision induced NSDI events, as shown in Fig. 3. For the recollision events, the electron pairs mainly distribute in the first and third quadrants [Figs. 3(a) and 3(c)], which is similar to the correlated electron momentum spectrum for the parallel aligned molecule with $R = 2$ a.u. While for the internal-collision NSDI events, the electron pairs for $R = 4$ a.u. are almost uniformly distributed in the four quadrants, and for $R = 6$ a.u. the distribution exhibits an obvious back-to-back emission behavior, as shown in Figs. 3(b) and 3(d). These results indicate that the internal-collision NSDI is responsible for the enhanced back-to-back emission for the parallel molecule at the large internuclear distances.

The difference in the correlated electron emissions for the recollision and internal-collision NSDI events can be understood by back tracing the classical trajectories. The sketches of these two types of NSDI are displayed in Figs. 4(a) and 4(b), respectively. The cyan solid line denotes the field-dressed potential for the parallel aligned molecule with $R = 6$ a.u. In this potential field, the electrons (black blobs) attached to the up-field and down-field cores can tunnel into the continuum through inner and outer potential barriers, respectively [38]. When the electron located at the down-field core tunnels through the outer barrier, it is accelerated along the laser polarization direction by the oscillating electric field and is impelled back to the parent molecular

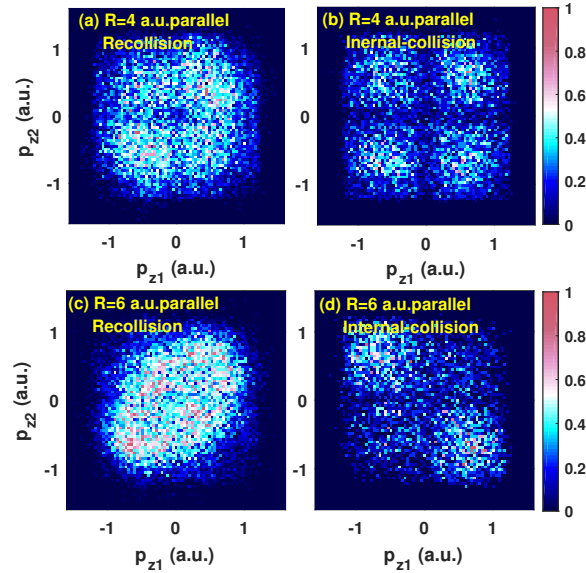


Fig. 3. Correlated electron momentum spectra along the laser polarization direction for the NSDI in the parallel aligned molecules with $R = 4$ a.u. (first row) and $R = 6$ a.u. (second row). The first and second columns correspond to the NSDI events occurring through recollision and internal collision, respectively. At $R = 4$ and 6 a.u., 15% and 34% of the NSDI events occur through the internal-collision process, respectively.

ion and knocks out the second electron, as shown in Fig. 4(a). This is the recollision NSDI. When the electron located at the up-field core tunnels through the inner barrier, it may move directly toward the down-field core, and kicks out the second electron. This is the internal-collision NSDI, as revealed in right column of Fig. 2.

We trace the NSDI trajectories and determine the recollision or collision time and the final double ionization time of the NSDI events. Figures 4(c) and 4(d) display the time delay between (re)collision and the ionization of the first electron for the recollision and internal-recollision NSDI events at $R=6$ a.u., respectively. Figures 4(e) and 4(f) show the time delay between double ionization and (re)collision for recollision and internal-recollision NSDI events, respectively. Here, for the recollision NSDI, the ionization time of the first electron (t_i) is defined as the moment when it achieves positive energy or is far away from the nearest nucleus more than 10 a.u. For the internal-collision NSDI, the ionization time of the first electron is defined as the instant when it moves across the center of the inner potential barrier. The (re)collision time (t_c) is defined as the instant of the closest approach of the two electrons and the double ionization time t_{DI} is defined as the moment when both electrons achieve positive energies. The energy of each electron contains the kinetic energy, potential energy of the electron-ion interaction and half of electron-electron repulsive energy. We mention that the following conclusions don't depend on the exact definitions of these quantities. One can see that for the recollision induced NSDI, the time delay between collision and the tunneling of the first electron peaks around $0.5T$ [Fig. 4(c)], while it is smaller than $0.15T$ for the internal collision induced NSDI events [Fig. 4(d)]. These statistic results support our statement of the recollision and internal-collision process above. For the internal collision, it only takes a very short time for the electron in the up-field core to move towards the down-field core.

For the time delay between double ionization and (re)collision, the two largest peaks locate around 0 and $0.25T$ for recollision induced NSDI [Fig. 4(e)]. For this time delay, the electron

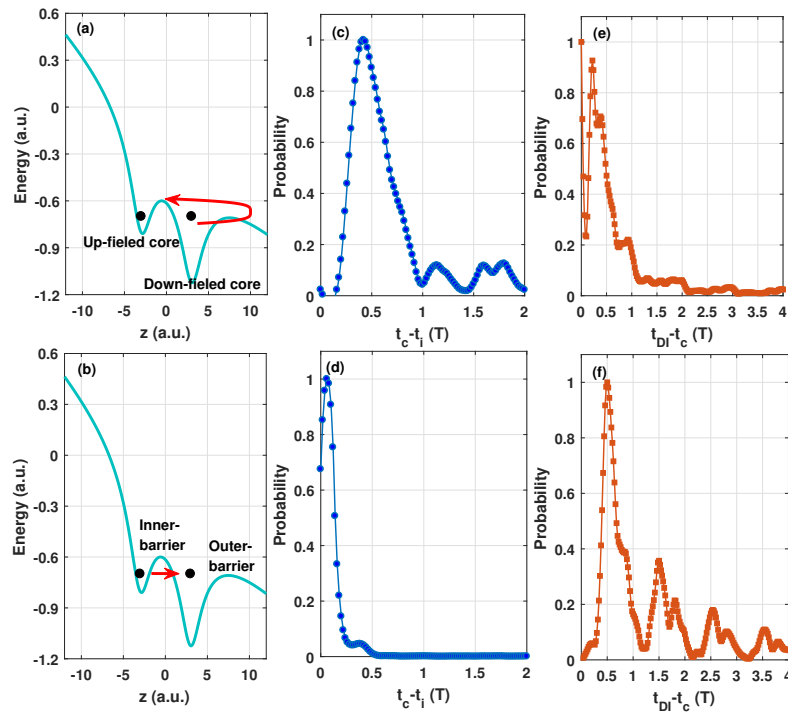


Fig. 4. Sketches of the recollision (a) and internal-collision (b) processes. (c) and (d) The time delay between (re)collision and the ionization of the first electron for the NSDI events in Figs. 3(c) and 3(d), respectively. (e) and (f) The time delay between double ionization and (re)collision for the NSDI events in Figs. 3(c) and 3(d), respectively.

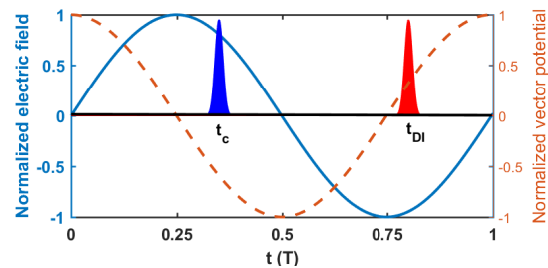


Fig. 5. A sketch of the collision time and double ionization time distributions for the NSDI events in Fig. 3(d). The blue solid and red dash curves represent the electric field and vector potential of the laser fields, respectively. The blue and red peaks denote the collision and double ionization times, respectively.

pairs are more likely to emit into the same hemisphere [8, 18], and thus the correlated electron momentum spectrum exhibits the dominant distribution in the first and third quadrants. However, for the internal-collision NSDI, the time delay distribution displays a prominent peak at $0.5T$, as shown in Fig. 4(f). For the internal collision, the collision occurs immediately after the first electron crosses the inner potential barrier of the molecule, which happens around the peak of the electric field, i.e., the collision occurs just after the electric field peak. Here, the $0.5T$ delay indicates that the second electron ionizes just after the next electric field peak after collision, as sketched in Fig. 5. Consequently, the two electrons possess opposite final momenta. This is the reason for the back-to-back emissions of the internal-collision NSDI events shown in Fig. 3(d).

For the recollision process, the returning energy could be as high as $3.2U_p$ (U_p is the ponderomotive potential), and thus the second electron could be excited to very high excited states or ionized directly after recollision. Therefore, the time delay between the recollision and double ionization is small. However, for the internal-collision process, the second electron could only be excited to low excited state because of the low collision energy. Thus, it stays in the excited state for a long time and is released when the subsequent peak of electric field arrives. It can be predicted that when the nuclear distance decreases, the collision energy further decreases and thus the second electron is ionized with a longer time delay. This is confirmed in Fig. 6, where we shown the time delay between double ionization and collision for the internal-collision NSDI at $R = 4$ a.u. It is shown that there are considerable NSDI events ionized with time delay much longer than $1.0T$. For this long time delay, the electron pairs could emit either into the same or opposite directions, depending on the time delay. Consequently, the final electron momentum spectrum exhibits an almost uniform distribution, as shown in Fig. 3(b).

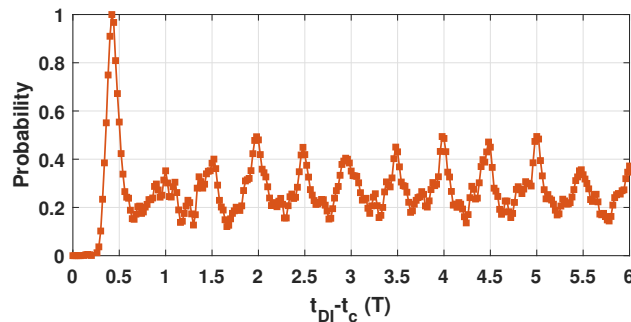


Fig. 6. The time delay between double ionization and collision for the NSDI events in Fig. 3(b).

4. Conclusions

In conclusion, we have investigated the alignment dependence of strong-field NSDI of molecules with different internuclear distances. The results show that at the small internuclear distance R , the electron pairs prefer to emit into the same hemisphere for the parallel alignment, as compared with perpendicularly aligned molecules. As R increases, the alignment-dependence of electron emission reverses, i.e., the electron pairs are more likely to emit into the opposite directions for the parallel aligned molecules. Classical trajectory analysis reveals that as R increases an internal-collision NSDI process appears. In this NSDI process, the first electron tunnels through the inner barrier from up-field core, moves directly towards the other nucleus to collide with the second electron, leading to the final ionization of the second electron. For the internal-collision NSDI, there is a relative long time delay between double ionization and collision because of the low collision energy. Thus the electron pairs are more possible to achieve final momenta with

opposite directions. This internal-collision NSDI does not appear in the perpendicularly aligned molecules. Therefore, the side-by-side emission of the electron pairs is more prevalence in the perpendicular molecules at larger internuclear distances.

Funding

National Natural Science Foundation of China (11547018, 11874163, 11622431, 61475055, 11604108, 11627809, 11404105) and Program for HUST Academic Frontier Youth Team.

References

1. A. l'Huillier, L. A. Lompre, G. Mainfray, and C. Manus, "Multiply charged ions induced by multiphoton absorption in rare gases at $0.53 \mu\text{m}$," *Phys. Rev. A* **27**(5), 2503-2512 (1983).
2. D. N. Fittinghoff, P. R. Bolton, B. Chang, and K. C. Kulander, "Observation of nonsequential double ionization of helium with optical tunneling," *Phys. Rev. Lett.* **69**(18), 2642-2645 (1992).
3. B. Walker, B. Sheehy, L. F. DiMauro, P. Agostini, K. J. Schafer, and K. C. Kulander, "Precision measurement of strong field double ionization of Helium," *Phys. Rev. Lett.* **73**(9), 1227-1230 (1994).
4. R. Moshhammer, B. Feuerstein, W. Schmitt, A. Dorn, C. D. Schröter, J. Ullrich, H. Rottke, C. Trump, M. Wittmann, G. Korn, K. Hoffmann, and W. Sandner, "Momentum distributions of Ne^{n+} ions created by an intense ultrashort laser pulse," *Phys. Rev. Lett.* **84**(3), 447-450 (2000).
5. A. Rudenko, K. Zrost, B. Feuerstein, V. L. B. de Jesus, C. D. Schröter, R. Moshhammer, and J. Ullrich, "Correlated multielectron dynamics in ultrafast laser pulse interactions with atoms," *Phys. Rev. Lett.* **93**(25), 253001 (2004).
6. R. Lafon, J. L. Chaloupka, B. Sheehy, P. M. Paul, P. Agostini, K. C. Kulander, and L. F. DiMauro, "Electron energy spectra from intense laser double ionization of Helium," *Phys. Rev. Lett.* **86**(13), 2762-2765 (2001).
7. J. L. Chaloupka, J. Rudati, R. Lafon, P. Agostini, K. C. Kulander, and L. F. DiMauro, "Observation of a transition in the dynamics of strong-field double ionization," *Phys. Rev. Lett.* **90**(3), 033002 (2003).
8. B. Feuerstein, R. Moshhammer, D. Fischer, A. Dorn, C. D. Schröter, J. Deipenwisch, J. R. Crespo Lopez-Urrutia, C. Höhr, P. Neumayer, J. Ullrich, H. Rottke, C. Trump, M. Wittmann, G. Korn, and W. Sandner, "Separation of recollision mechanisms in nonsequential strong field double ionization of Ar: the role of excitation tunneling," *Phys. Rev. Lett.* **87**(4), 043003 (2001).
9. R. Moshhammer, J. Ullrich, B. Feuerstein, D. Fischer, A. Dorn, C. D. Schröter, J. R. Crespo, López-Urrutia, C. Höhr, H. Rottke, C. Trump, M. Wittmann, G. Korn, K. Hoffmann, and W. Sandner, "Strongly directed electron emission in non-sequential double ionization of Ne by intense laser pulses," *J. Phys. B* **36**(6), L113-L119 (2003).
10. P. B. Corkum, "Plasma perspective on strong field multiphoton ionization," *Phys. Rev. Lett.* **71**(13), 1994-1997 (1993).
11. K. J. Schafer, B. Yang, L. F. DiMauro, and K. C. Kulander, "Above threshold ionization beyond the high harmonic cutoff," *Phys. Rev. Lett.* **70**(11), 1599-1602 (1993).
12. J. Tan, Y. Zhou, M. He, Y. Chen, Q. Ke, J. Liang, X. Zhu, M. Li, and P. Lu, "Determination of the ionization time using attosecond photoelectron interferometry," *Phys. Rev. Lett.* **121**(25), 253203 (2018).
13. X. Zhang, X. Zhu, D. Wang, L. Li, X. Liu, Q. Liao, P. Lan, and P. Lu, "Ultrafast oscillating-magnetic-field generation based on electronic-current dynamics," *Phys. Rev. A* **99**(2), 013414 (2019).
14. A. Staudte, C. Ruiz, M. Schöffler, S. Schössler, D. Zeidler, Th. Weber, M. Meckel, D. M. Villeneuve, P. B. Corkum, A. Becker, and R. Dörner, "Binary and recoil collisions in strong field double ionization of helium," *Phys. Rev. Lett.* **99**(26), 263002 (2007).
15. A. Rudenko, V. L. B. de Jesus, Th. Ergler, K. Zrost, B. Feuerstein, C. D. Schröter, R. Moshhammer, and J. Ullrich, "Correlated two-electron momentum spectra for strong-field nonsequential double ionization of He at 800 nm," *Phys. Rev. Lett.* **99**(26), 263003 (2007).
16. Y. Liu, S. Tschuch, A. Rudenko, M. Dürr, M. Siegel, U. Morgner, R. Moshhammer, and J. Ullrich, "Strong-field double ionization of Ar below the recollision threshold," *Phys. Rev. Lett.* **101**(5), 053001 (2008).
17. C. Figueira de Morisson Faria, H. Schomerus, X. Liu, and W. Becker, "Electron-electron dynamics in laser-induced nonsequential double ionization," *Phys. Rev. A* **69**(4), 043405 (2004).
18. S. L. Haan, J. S. Van Dyke, and Z. S. Smith, "Recollision excitation, electron correlation, and the production of high-momentum electrons in double ionization," *Phys. Rev. Lett.* **101**(11), 113001 (2008).
19. D. Ye, X. Liu, and J. Liu, "Classic trajectory diagnosis of a fingerlike pattern in the correlated electron momentum distribution in strong field double ionization of Helium," *Phys. Rev. Lett.* **101**(23), 233003 (2008).
20. A. S. Alnaser, D. Comtois, A. T. Hasan, D. M. Villeneuve, J. Kieffer, and I. V. Litvinyuk, "Strong-field non-sequential double ionization: wavelength dependence of ion momentum distributions for neon and argon," *J. Phys. B* **41**(3), 031001 (2008).
21. O. Herrwerth, A. Rudenko, M. Kremer, V. L. B. de Jesus, B. Fischer, G. Gademann, K. Simeonidis, A. Achtelik, Th. Ergler, B. Feuerstein, C. D. Schröter, R. Moshhammer and J. Ullrich, "Wavelength dependence of sub-laser-cycle few-electron dynamics in strong-field multiple ionization," *New J. Phys.* **10**(2), 025007 (2008).
22. A. D. DiChiara, E. Sistrunk, C. I. Blaga, U. B. Szafruga, P. Agostini, and L. F. DiMauro, "Inelastic scattering of broadband electron wave packets driven by an intense midinfrared laser field," *Phys. Rev. Lett.* **108**(3), 033002 (2012).

23. B. Wolter, M. G. Pullen, M. Baudisch, M. Sclafani, M. Hemmer, A. Senftleben, C. D. Schröter, J. Ullrich, R. Moshhammer, and J. Biegert, "Strong-field physics with mid-IR fields," *Phys. Rev. X* **5**(2), 021034 (2015).
24. Y. Wang, S. Xu, W. Quan, C. Gong, X. Lai, S. Hu, M. Liu, J. Chen, and X. Liu, "Recoil-ion momentum distribution for nonsequential double ionization of Xe in intense midinfrared laser fields," *Phys. Rev. A* **94**(5), 053412 (2016).
25. X. Ma, Y. Zhou, and P. Lu, "Multiple recollisions in strong-field nonsequential double ionization," *Phys. Rev. A* **93**(1), 013425 (2016).
26. Q. Li, Y. Zhou, and P. Lu, "Universal time delay in the recollision impact ionization pathway of strong-field nonsequential double ionization," *J. Phys. B* **50**(22), 225601 (2017).
27. X. Ma, Y. Zhou, N. Li, M. Li, and P. Lu, "Attosecond control of correlated electron dynamics in strong-field nonsequential double ionization by parallel two-color pulses," *Optics and Laser Technology* **108**, 235-240 (2018).
28. C. Huang, M. Zhong, and Z. Wu, "Anomalous ellipticity dependence in nonsequence double ionization of ArXe," *Sci. Rep.* **8**, 8772 (2018).
29. X. Ma, Y. Zhou, Y. Chen, M. Li, Y. Li, Q. Zhang, and P. Lu, "Timing the release of the correlated electrons in strong-field nonsequential double ionization by circularly polarized two-color laser fields," *Opt. Express* **27**(3), 1825-1837 (2019).
30. E. Eremina, X. Liu, H. Rottke, W. Sandner, M. G. Schätzel, A. Dreischuh, G. G. Paulus, H. Walther, R. Moshhammer, and J. Ullrich, "Influence of molecular structure ionization of N₂ and O₂ by high intensity ultrashort laser pulses," *Phys. Rev. Lett.* **92**(17), 173001 (2004).
31. A. S. Alnaser, S. Voss, X. M. Tong, C. M. Maharjan, P. Ranitovic, B. Ulrich, T. Osipov, B. Shan, Z. Chang, and C. L. Cocke, "Effects of molecular structure on ion disintegration patterns in ionization of O₂ and N₂ by short laser pulses," *Phys. Rev. Lett.* **93**(11), 113003 (2004).
32. J. S. P. Bechcicki, K. Sacha, B. Eckhardt, and J. Zakrzewski, "Nonsequential double ionization of molecules," *Phys. Rev. A* **71**(3), 033407 (2005).
33. D. Zeidler, A. Staudte, A. B. Bardon, D. M. Villeneuve, R. Dörner, and P. B. Corkum, "Controlling attosecond double ionization dynamics via molecular alignment," *Phys. Rev. Lett.* **95**(20), 203003 (2005).
34. C. Huang, Y. Zhou, A. Tong, Q. Liao, W. Hong, and P. Lu, "The effect of molecular alignment on correlated electron dynamics in nonsequential double ionization," *Opt. Express* **19**(6), 5627-5634 (2011).
35. T. Zuo, and A. D. Bandrauk, "Charge-resonance-enhanced ionization of diatomic molecular ions by intense lasers," *Phys. Rev. A* **52**(4), R2511 (1995).
36. Tamer Seideman, M. Yu. Ivanov, and P. B. Corkum, "Role of electron localization in intense-field molecular ionization," *Phys. Rev. Lett.* **75**(15), 2819-2822 (1995).
37. Y. Qin, M. Li, Y. Li, M. He, S. Luo, Y. Liu, Y. Zhou, and P. Lu, "Asymmetry of the photoelectron momentum distribution from molecular ionization in elliptically polarized laser pulses," *Phys. Rev. A* **99**(1), 013431 (2019).
38. J. Wu, M. Meckel, L. Ph. H. Schmidt, M. Kunitski, S. Voss, H. Sann, H. Kim, T. Jahnke, A. Czasch, and R. Dörner, "Probing the tunnelling site of electrons in strong field enhanced ionization of molecules," *Nat. Commun.* **3**(4), 1113 (2012).
39. X. Gong, Q. Song, Q. Ji, H. Pan, J. Ding, J. Wu, and H. Zeng, "Strong-field dissociative double ionization of Acetylene," *Phys. Rev. Lett.* **112**(24), 243001 (2014).
40. E. Dehghanian, A. D. Bandrauk, and G. L. Kamta, "Enhanced ionization of the H₂ molecule driven by intense ultrashort laser pulses," *Phys. Rev. A* **81**(6), 061403(R) (2010).
41. J. S. Parker, B. J. S. Doherty, K. T. Taylor, K. D. Schultz, C. I. Blaga, and L. F. DiMauro, "High-energy cutoff in the spectrum of strong-field nonsequential double ionization," *Phys. Rev. Lett.* **96**(13), 133001 (2006).
42. S. Hu, "Boosting photoabsorption by attosecond control of electron correlation," *Phys. Rev. Lett.* **111**(12), 123003 (2013).
43. S. L. Haan, L. Breen, A. Karim, and J. H. Eberly, "Variable time lag and backward ejection in full-dimensional analysis of strong-field double ionization," *Phys. Rev. Lett.* **97**(10), 103008 (2006).
44. S. L. Haan, Z. S. Smith, K. N. Shomsky, and P. W. Plantinga, "Electron drift directions in strong-field double ionization of atoms," *J. Phys. B* **42**(13), 134009 (2009).
45. X. Wang, and J. H. Eberly, "Elliptical trajectories in nonsequential double ionization," *New J. Phys.* **12**(9), 093047 (2010).
46. L. Fu, J. Liu, J. Chen, and S. Chen, "Classical collisional trajectories as the source of strong-field double ionization of helium in the knee regime," *Phys. Rev. A* **63**(4), 043416 (2001).
47. F. Mauger, C. Chandre, and T. Uzer, "Recollisions and correlated double ionization with circularly polarized light," *Phys. Rev. Lett.* **105**(8), 083002 (2010).
48. Y. Zhou, Q. Liao, and P. Lu, "Asymmetric electron energy sharing in strong-field double ionization of helium," *Phys. Rev. A* **82**(5), 053402 (2010).
49. Y. Zhou, C. Huang, Q. Liao, and P. Lu, "Classical simulations including electron correlations for sequential double ionization," *Phys. Rev. Lett.* **109**(5), 053004 (2012).
50. Y. Zhou, M. Li, Y. Li, A. Tong, Q. Li, and P. Lu, "Dissection of electron correlation in strong-field sequential double ionization using a classical model," *Opt. Express* **25**(7), 8450-8458 (2017).
51. Y. Zhou, C. Huang, A. Tong, Q. Liao, and P. Lu, "Correlated electron dynamics in nonsequential double ionization by orthogonal two-color laser pulses," *Opt. Express* **19**(3), 2301-2308 (2011).
52. L. Zhang, X. Xie, S. Roither, Y. Zhou, P. Lu, D. Kartashov, M. Schöffler, D. Shafir, P. B. Corkum, A. Baltuška, A.

- Staudte, and M. Kitzler, "Subcycle control of electron-electron correlation in double ionization," *Phys. Rev. Lett.* **112**(19), 193002 (2014).
53. A. Tong, Y. Zhou, and P. Lu, "Resolving subcycle electron emission in strong-field sequential double ionization," *Opt. Express* **23**(12), 15774-15783 (2015).
54. M. S. Schöffler, X. Xie, P. Wustelt, M. Möller, S. Roither, D. Kartashov, A. M. Sayler, A. Baltuska, G. G. Paulus, and M. Kitzler, "Laser-subcycle control of sequential double-ionization dynamics of helium," *Phys. Rev. A* **93**(6), 063421 (2016).
55. Phay J. Ho, R. Panfili, S. L. Haan, and J. H. Eberly, "Nonsequential double ionization as a completely classical photoelectric effect," *Phys. Rev. Lett.* **94**(9), 093002 (2005).
56. T. -T. Nguyen-Dang, F. Châteauneuf, and S. Manoli, "Tunnel ionization of H₂ in a low-frequency laser field: A wave-packet approach," *Phys. Rev. A* **56**(3), 2142-2167 (1997).